STUDIES ON MECHANICAL AND DIELECTRIC PROPERTIES OF NATURAL RUBBER–REDUCED GRAPHENE OXIDE NANOCOMPOSITES

[1]Jophy Jose, [2]Susamma A. P

[1]Research Scholar, [2]Director, Planning, KUFOS

[1]Department of Chemistry

[1]Maharaja's College Ernakulam, Kerala, India -682011.

Abstract: A series of Natural Rubber- Reduced Graphene Oxide (NR- RGO) nanocomposites with varying compositions of RGO were prepared by latex mixing method. RGO, prepared by the reduction of GO using hydrazine hydrate was characterised by FTIR, UV, SEM, TEM and XRD studies. The successful incorporation of RGO into the NR matrix was analysed by SEM and XRD studies. Mechanical property studies of NR- RGO nanocomposites conducted revealed that the successful incorporation of RGO into the NR latex showed multifunctional properties as well as enhanced mechanical properties like tensile strength, tensile modulus, tear strength etc. Nanocomposite with 0.1 phr of RGO incorporated NR was optimised as the best composition compared to other compositions (0.03,0.05,0.075,0.3,0.5, and 1.0 phr) in terms of mechanical properties. The presence of RGO can also enhance the dielectric properties of NR nanocomposites.

Key words: nanocomposites, natural rubber, graphene oxide, reduced graphene oxide.

1. INTRODUCTION

Reinforcing natural rubbers with various fillers is a common strategy because unfilled rubbers have very limited application due to their poor mechanical properties [1]. During earlier days, Carbon Black and Silica are the common reinforcing fillers [2,3]. Recent advancement in nanotechnology have resulted in the realization of some new nanofillers due to the fact that these nanofillers could not only improve the mechanical properties of rubbers at very low loading, but also imparts some new functionalities to the rubbers, for eg. electrical conductivity, wear resistance, low gas permeability and low heat buildup [4,5,6]. Graphene, one atom thick nano sheet comprised of SP^2 hybridized carbon atoms attains more interest in the area of polymer- nanocomposites during the past few years due to excellent characteristics such as electrical, mechanical, optical properties etc [7]. Thus Graphene commonly known as Reduced Graphene Oxide (RGO) can be considered as an ideal nanofiller for Natural Rubber (NR) owing to its ability to impart prominent mechanical and multifunctional properties, provided that fine dispersion and strong interfacial interaction can be achieved [7,8,9,10]. For first time, Prud' Homme et al and Ozbas et al added thermally-reduced graphene into several elastomers including natural rubber, styrene butadiene rubber and poly (dimethyl Siloxane) [11,12]. These work demonstrated the prominent potential of graphene in improving the mechanical and gas barrier properties of elastomers. Tang et al and Zhan et al fabricated graphene based rubber nanocomposites with a conductive segregated network exhibiting good electrical conductivity and water vapour impermeability [13,14]. Also graphene was found to be effective in improving the thermal stability and abrasion resistance. Hence graphene has attracted increasing interest in functional rubber nanocomposites [15].

The present study aims to synthesise reduced Graphene oxide and it was characterised by FTIR, Raman, XRD, TEM and SEM measurements. Then NR-RGO nanocomposites of varying compositions were prepared by latex mixing method and characterised by XRD analysis. The morphological studies of the nanocomposites were done by SEM measurements and its mechanical and dielectric property studies were conducted and compared with that of NR-GO nanocomposite.

2. EXPERIMENTAL

2.1 Materials

NR latex used for the study was centrifuged NR latex, purchased from Njavallil latex, Cochin, India. The composition and properties are given in table1

Table1 Composition and properties of NR latex

Dry rubber content,	% by mass	60.04
Total solid content,	% by mass	61.05
Coagulum content,	% by mass	00.03
Sludge content,	% by mass	0.004
Alkalinity as ammonia,	% by mass	00.73
KOH number		00.65
Mechanical stability time, sec		1075
Volatile fatty acid number		0.04
Copper content		Traces
Manganese content		Traces

Graphite Powder 150 micron was purchased from Nice chemicals. The other reagents zinc oxide (ZnO), sulphur, zinc diethyl di thiocarbamate (ZDC), potassium oleate, potassium butyl xanthate, sulphuric acid (H_2SO_4), sodium nitrate ($NaNO_3$), Potassium permanganate ($KMnO_4$), Hydrogen peroxide (H_2O_2), Ammonia (NH_3) and hydrazine hydrate (H_6N_2O) were purchased from Merck Specialities Private Ltd, Mumbai, India.

2.2 Preparation of graphene oxide (GO)

Modified Hummers method was used to synthesize GO [16]. 150 ml H_2SO_4 & 5 g $NaNO_3$ were stirred for 15 minutes in an ice bath. Then 5 g graphite powder was added within 10 minutes. After half an hour, 15 g $KMnO_4$ was added slowly within half an hour. Stirred the mixture for 30 minutes. During this time the temperature of the suspension was maintained at 35 to 40^0 C. After cooling added 200 ml water drop by drop with continuous stirring. Then added 5 ml 30% H_2O_2 to the suspension, till the colour of the suspension changed yellow. The suspension was washed with distilled water several times till the P^H of the solution is neutral. The final product, GO, was dried at 60^0 C under vacuum for 12 hours.

2.3 Preparation of reduced graphene oxide (RGO)

Pre calculated amount of GO (1g) powder as obtained by Modified Hummers method was mixed with 250 ml of water in a beaker and sonicated vigorously for 30 minutes to prepare the colloidal solution. 5 ml of hydrazine hydrate was added to the solution and poured into the soxhlet apparatus mantle. The round bottom flask was set to heating to 100^0C in an oil bath, set in a watercooled condenser for 24 hours, over which the reduced GO gradually precipitated out as a black solid. The product was isolated by filtration and washed with water and dried and named it as Reduced Graphene Oxide (RGO) [17].

2.4 Preparation of NR/RGO Nanocomposites:

For the preparation of the composite latex mixing method is used. During compounding of latex, the solid ingredients were added into latex as solutions or dispersions.

2.4.1 De-ammoniation of latex: High ammonia type concentrated latex was de–ammoniated to 0.23% by stirring in a laboratory type de–ammoniation tank for 3 hrs. Otherwise the high ammonia content in latex will create problems during conversion to solid products or in the stability of the latex, compound in presence of Zinc oxide. The concentration of ammonia in latex was estimated as per ASTMD1076-88.

2.4.2 Mixing of Ingredients: The aqueous dispersions of RGO were prepared followed by sonication for optimum time (60 minutes at 30 w) and these dispersions were mixed with NR latex so as to get RGO concentrations ranging from 0 - 1 phr in NR. The mixing of ingredients was done as per the order given in the table 1. The stabilizers were first added as solutions, followed by the other ingredients. Mixing was done in a glass vessel and stirring for homogenization was done using a laboratory stirrer at 10 - 20 rpm. It was occasionally stirred during storage also in order to prevent settling of the ingredients.

2.4.3 Maturation: The latex compound was matured at ambient temperature for 24 hours. This ensures the compound to free itself of air entrained during the preparation and allows the stabilizers to distribute themselves uniformly throughout the aqueous and dispersed media. During this maturation period important changes take place. Absorption of vulcanisation ingredients into the rubber particle surface commences and becomes a continuous process with time and temperature. Further it allows time for the reaction of ammoniated latex with ZnO for getting uniform physico – chemical properties.

2.4.4 *Preparation of Latex films:* Latex films were cast on glass dishes using the latex compound as described by Flint and Naunton [18]. The size of the glass dishes was 6" x 6" and about 25 ml of the latex compound was poured and uniformly distributed so that a film of thickness 1 – 1.25 mm was obtained upon drying. These glass dishes with the latex compound were placed on leveled tables and dried overnight.

2.4.5 Vulcanisation of latex films:The vulcanisation of latex films was carried out in a laboratory type air oven at 100^0 C. The time for optimum curve was determined by vulcanising the film for different duration of time and determining the tensile strength of the vulcanisate in each case. The optimum cure time was taken as the time for attaining maximum tensile strength. Thus the rubber nanocomposites were developed by incorporating the nanofiller (RGO) synthesized in natural rubber latex as per the formulations given below.

Table 2: Formulation of NR – RGO composites

Ingredients	1	2	3	4	5	6	7	8
	Wet weight in grams							
60% centrifuged NR Latex	167	167	167	167	167	167	167	167
10% KOH	2.5	2.5	2.5	2.5	2.5	2.5	2.5	2.5
10% Potassium Oleate solution	1	1	1	1	1	1	1	1
50% Sulphur dispersion	2.5	2.5	2.5	2.5	2.5	2.5	2.5	2.5
50 % ZDC dispersion	2	2	2	2	2	2	2	2
50% ZnO dispersion	1	1	1	1	1	1	1	1
Potassium Butyl Xanthate	2	2	2	2	2	2	2	2
RGO in phr	0	0.03	0.05	0.075	0.1	0.3	0.5	1.0

2.5 Characterisation

Scanning electron microscopy (SEM, JEOL Model JSM 6390 LV) was used to characterise the morphology of GO and also the NR–GO nanocomposites. The X-ray diffraction patterns were employed to portray the structure of GO. FTIR is an excellent analytical tool used to determine the structure and functional groups in a molecule. FTIR is useful in detecting the characteristic vibrational frequencies of molecules. Tensile and tear properties are studied by using a universal testing machine. Dielectric and AC conductivity studies in the frequency range 40 Hz to 30 MHz were done using Precision Impedance Analyser (Agilent 4294A) with dielectric text fixture 16451B. Transmission electron microscope analysis was performed using a JEM-2100F TEM with an accelerating voltage of 200 keV.

3. RESULTS AND DISCUSSION

3.1 Characterisation of reduced graphene oxide

3.1.1 X-ray Diffraction (XRD)

Fig (1) shows the XRD of RGO which showsno clear diffraction peak in its XRD pattern. The absence of intense peaks at 10° which corresponds to GO and 25° corresponding to graphite clearly confirms the conversion of GO to RGO [19]. Unlike GO, RGO has a very weak and broad peak centered at 2θ = 25–30 degree corresponding to increased d spacing which might be attributed to very thin RGO layers due to high degree of exfoliation. The close d-spacing of RGO to pristine graphite and disappearance of peak at 2θ = 10 degree indicate that the oxygen containing functional groups of graphene oxide have been successfully removed. There are published data which report that the graphene nanosheets are exfoliated into a monolayer or few-layers and it results in new lattice structure, which is significantly different from the pristine graphite flakes and graphene oxide.The diffraction peak of RGO is so weak that it cannot be visible when drawn together in the XRD pattern with graphite and GO.

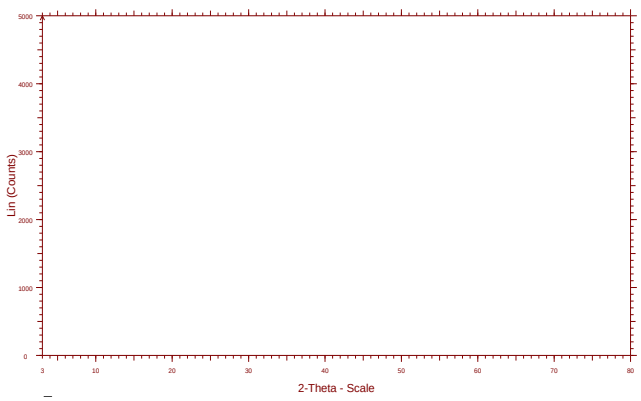

Fig. (1) XRD of RGO

3.1.2 Fourier Transform Infra-Red Spectroscopy (FTIR)

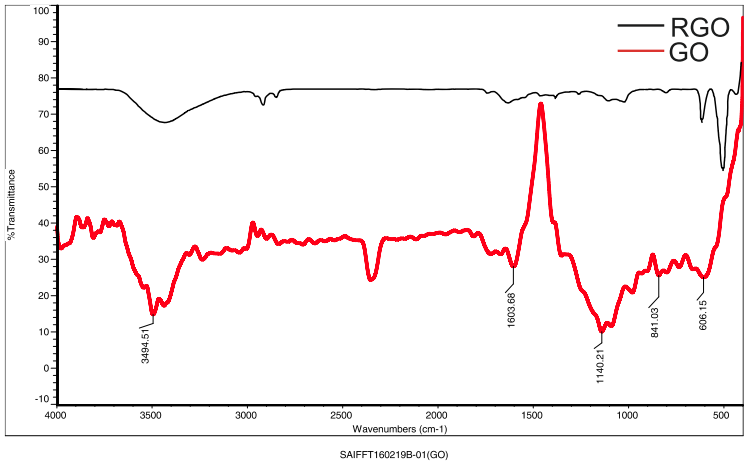

Fig (2) FTIR spectrum of GO and RGO

Fig (2) shows the FTIR spectrum of GO and RGO. Fig (2) shows the FTIR spectrum of RGO. The FTIR spectrum of GO reveals several molecular vibrational frequencies for GO indicating the presence of hydroxyl (-OH), carbonyl (-C=O) and epoxy groups (C-O-C). After the process of reduction, the oxygen containing groups were eliminated or the intensity of the peak is decreased as in the case of epoxy group. The functional groups present in the GO spectrum were reduced significantly in the RGO spectra. But the conjugated π systems are restored. So this confirms the conversion of GO to RGO. [20]. Characteristic peaks observed in the GO spectrum including C–OH (1160 cm^{-1}), O–H (3494 cm^{-1}) and C = O (1720 cm^{-1}) observed in the GO spectrum were significantly reduced in the RGO spectra. This clearly indicated the loss of oxygen groups form GO suggesting the formation of RGO. Here the absorption due to the C=O group (1720 cm^{-1}) is found to be decreased very much in intensity which confirms the removal of carboxylic group upon reduction. An absorption band that appears at 1583 cm^{-1} may be attributed to the skeletal vibration of the reduced graphene oxide [9]. The absence of obvious peaks in the spectrum indicates the complete reduction of GO to RGO. Some of the carbon-oxygen functional groups even existed, but their characteristic peaks are just very weak [19,20].

3.1.3 UV – VIS spectroscopy

UV-VIS spectroscopy is carried out to study the electronic absorption of reduced graphene oxide films. Figure (3) shows the UV-VIS spectrum of reduced graphene oxide. The UV-VIS spectrum of GO showed two absorption peaks at wavelengths of 234 nm and 301nm which correspond to C-C and C=O molecular absorption, respectively [18]. After reduction the C=O peak disappears, and C-C peak is recorded at wavelength of 265 nm [19].

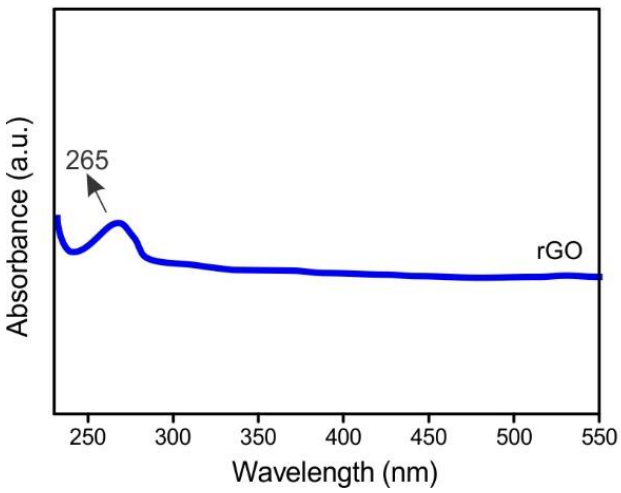

Fig (3) UV-VIS spectrum of RGO

3.2 Morphological Analysis

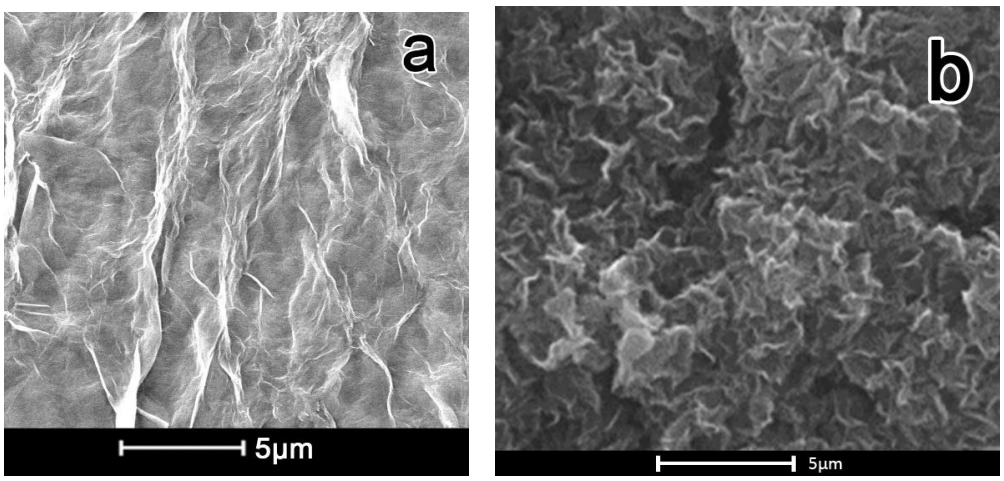

Fig (4) SEM images of (a) GO (b) RGO

The morphological and structural properties of RGO nanosheets were analysed through SEM and TEM observations. The SEM image of RGO reveals the graphene nanostructure with a smaller distance between the planes due to reduction by which compression and removal of oxygen functional groups takes place. [22]. The RGO flakes appear to be irregularly folded layered structure which may be because of deformation caused by the reduction and restacking processes [14]. The TEM image shows the presence of more wrinkles and crumples on RGO surface which was the result of negative thermal expansion of RGO. [23]. Thus the morphological difference of RGO from GO again confirms the above results.

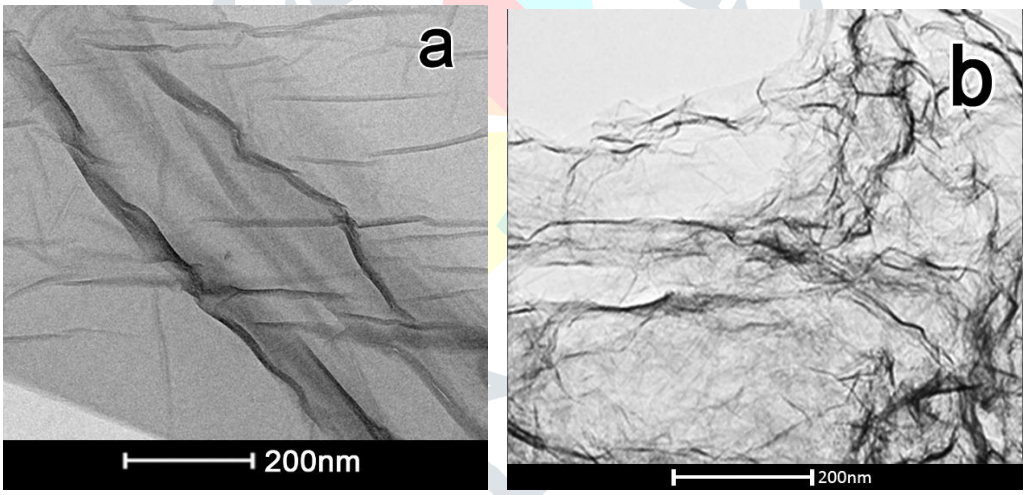

Fig (5) TEM images of (a) GO (b) RGO

3.3 Characterisation of NR-RGO nanocomposites

3.3.1 X ray diffraction analysis

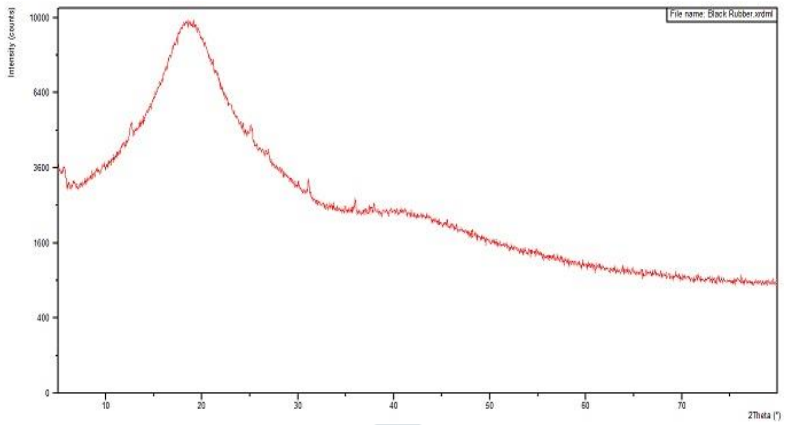

Fig (6) XRD of NR- RGO nanocomposite

XRD pattern of NR- RGO nanocomposites in fig. (6) shows no detectable characteristic peaks of graphite or GO, which further confirms that there is no significant layer –by- layer restack of RGO [24].

3.4 Analysis of Morphology of NR-GO nanocomposites

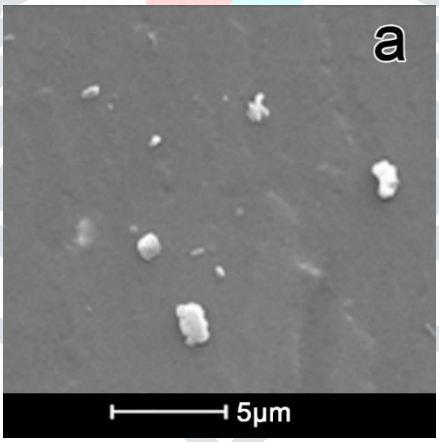

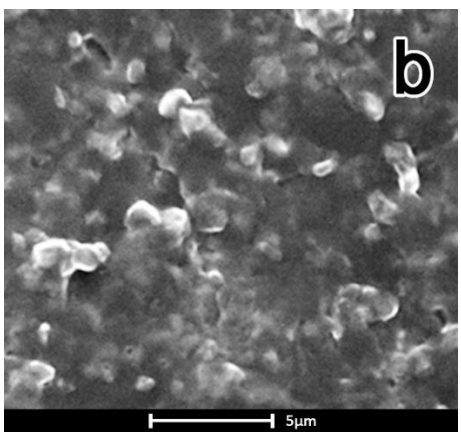

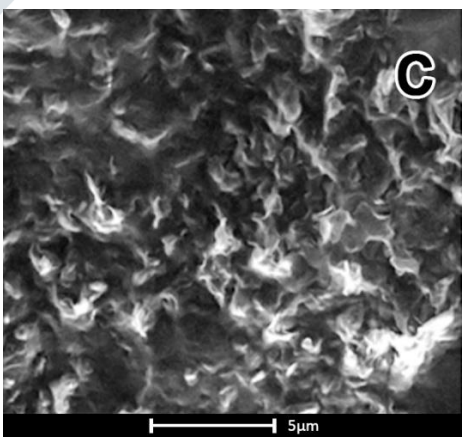

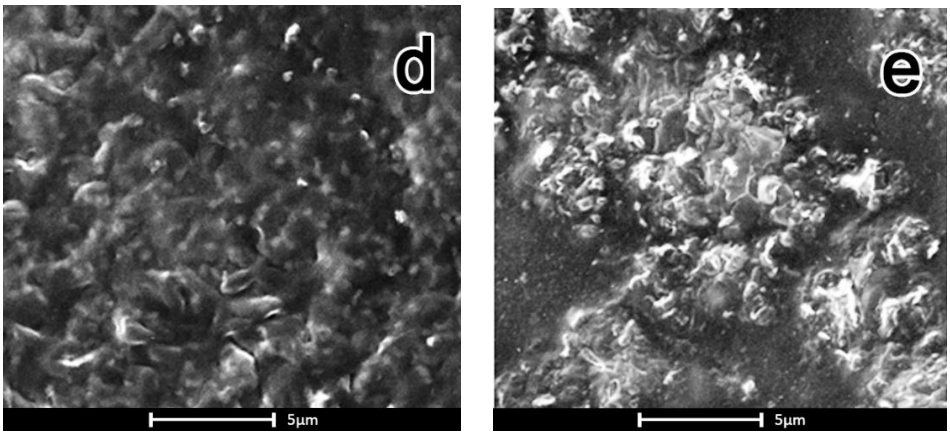

Fig (7) SEM micrographs of NR-RGO nanocomposites. Tensile fractured surface of (a) NR (b) NR- 0.05 RGO (c) NR-0.1 RGO (d) NR-0.5 RGO (e) NR-1.0 RGO

The dispersion of RGO in NR matrix is crucial to determine the final performance of nanocomposites [21]. Fig.1 shows the morphological structure of NR-RGO nanocomposites. The SEM measurements show that the RGO was well distributed as single layers in the NR latex. This suggests that the latex mixing technique is an effective method to obtain nanocomposites with well dispersed RGO in the NR matrix. The enhancement in mechanical and dielectric properties of the nanocomposites depend mainly on the well dispersion of RGO in NR matrix. However, the surface of the NR-RGO nanocomposites is very rough compared with unfilled NR. The roughness of the surface of the nanocomposites increases with the content of RGO in the NR matrix. The roughness of the surface of the NR-RGO nanocomposite enhances its mechanical properties. RGO is found to be well dispersed in the NR matrix for the nanocomposites with 0.1 phr RGO. Here good adhesion of RGO to the NR matrix is observed. As the content of RGO increased to 0.5 phr, more nanoparticles have appeared on the observing surface. RGO still showed somewhat good dispersion, and some connections were found between the neighbouring nanoparticles. For the nanocomposites with 1.0 phr RGO, the aggregation of nanoparticles could be seen from the figure. Here the RGO particles were stacked to form larger aggregates and NR latex was observed in the space between them. These aggregates will act as the stress concentration points when force is applied and reduces the tensile strength and modulus.

3.5 Mechanical properties

Stress-strain graph of NR –RGO nanocomposites are shown in fig.8. The numbers in the fig. indicates the RGO loading in the nanocomposites. The stress increases with RGO loading from 0.03 phr to 1 phr for any given strain. Mechanical properties of NR- GO ,NR RGO nanocomposites prepared through latex stage mixing are given in Table 3 and 4 respectively. It is clear from the results that RGO was remarkably effective in reinforcing NR.

Table 3: Mechanical properties of NR, NR-GO composites

Sl. No.	Formulations	Tensile strength (N/mm^2)	Elongation at break (%)	Tensile modulus at 300% elongation (N/mm^2)	Tear strength(N/mm)
1	NR	21.0	1690	1.05	34.5
2	NR+.03phr GO	28	1790	1.89	45.5
3	NR+0.05 phr GO	29.2	1810	1.65	47.3
4	NR+.075phr GO	30.1	1819	1.79	49.8
5	NR+0.1 phr GO	34.8	1798	1.92	52.5
6	NR+0.3 phr GO	33.7	1766	1.70	48.3
7	NR+.5phr GO	32.1	1745	1.65	47.4
8	NR+1 phr GO	29.5	1725	1.45	46.8

Table 4: Mechanical properties of NR, NR-RGO nanocomposites

Sl. No.	Formulations	Tensile strength (N/mm^2)	Elongation at break (%)	Tensile modulus at 300% elongation (N/mm^2)	Tear strength (N/mm)
1	NR	21.0	1690	1.05	34.5
2	NR+0.03phr RGO	28.5	1698	1.59	49.9
3	NR+0.05 phrRGO	29.9	1712	1.64	51.3
4	NR+0.075 phrRGO	30.6	1730	1.82	53.9
5	NR+0.1 phr RGO	35.4	1735	1.93	55.8
6	NR+0.3 phr RGO	34.2	1730	1.89	54.2
7	NR+0.5phr RGO	33.5	1721	1.78	53.7
8	NR+1.0phr RGO	32.8	1718	1.69	52.8

The tensile strength of NR has been improved by almost 69%, tensile modulus (300% elongation) by 84% and tear strength by 62% on addition of 0.1 phr of RGO which is greater than that of adding 0.1phr GO. In the case of GO, the increase in tensile strength, tensile modulus and tear strength are 66%, 83% and 52% respectively. In both cases beyond the loading of 0.1 phr further improvement in properties does not occur, which may be due to the agglomeration of the filler. The enhanced mechanical property is due to the relatively good dispersion of RGO in the NR matrix than GO. Recently, Zhang and Coworkers [25] proposed a percolation theory to describe the relationship between the tensile strength and the filler loading. According to this theory the percolation point of the nanocomposites took place at an extremely low filler content. The elongation at break is higher than NR for all the RGO composites indicating the strong interaction of RGO with the rubber matrix.

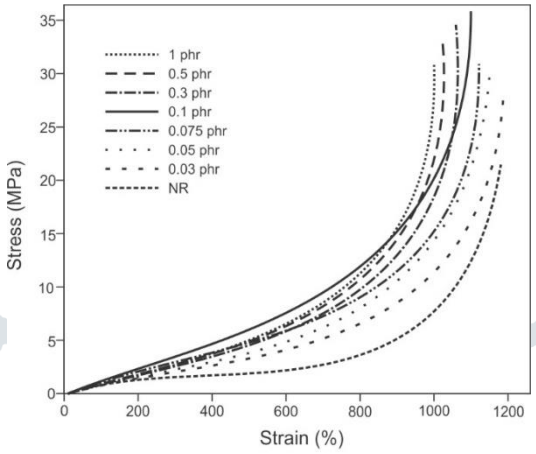

Fig (8) Stress-strain behavior of NR nanocomposites at different concentrations of RGO

3.6 Dielectric properties

The fig. 9 and 10 shows frequency dependence of AC conductivity, dielectric constant and dielectric loss of the NR- GO and NR- RGO nanocomposites respectively at room temperature. Both dielectric constant and dielectric loss values are high at low frequency and then decrease exponentially with increase in frequency. There is a remarkable increase in the dielectric constant from 4.8 for pure NR to approximately 1070 at 100 Hz for 1.0 phr NR- RGO nanocomposites and that for 1.0 phr NR-GO nanocomposite it increases to approximately 100. If this material is exposed to electromagnetic plane waves, the electric dipole moments created per unit volume will be higher. This will result in a high dielectric constant and dielectric loss at lower frequencies. As the frequency increases the induced dielectric polarisability will decrease, which can result in a reduction in both properties. An opposite effect is observed in the conductivity of the material ie. conductivity increases with increase in frequency. The conductivity reached a value of 10-4 S/m at 107Hz for 1.0 phr NR- RGO nanocomposite which is higher than that of 1.0 phr NR- GO nanocomposite. This observation may be due to the nano dimensions of RGO compared to GO and the relatively good dispersion of RGO in the NR matrix coupled with their superior pi – pi interactions. The oxygen functionalisation on GO may be another reason for its reduced electrical conductivity. At higher frequencies the external electromagnetic field will induce surface current within the material and the conduction will be dominated by the conduction current, whereas at lower frequencies conduction will be enabled by the displacement currents associated with the dipole moments created. But the ohmic loss associated with the conduction current will be lower as compared to the loss offered by the electric dipole moments and hence the dielectric loss is higher at low frequencies [26,27,28].

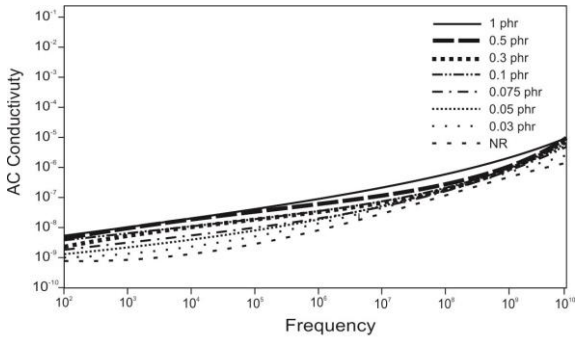

(a)

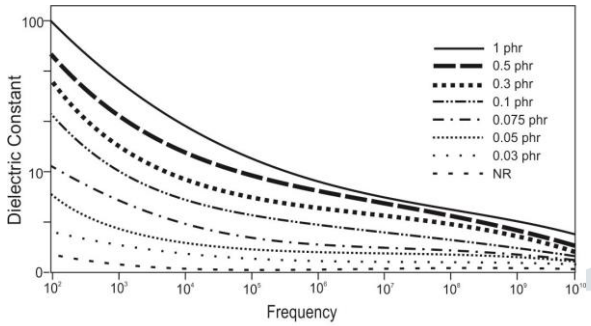

(b)

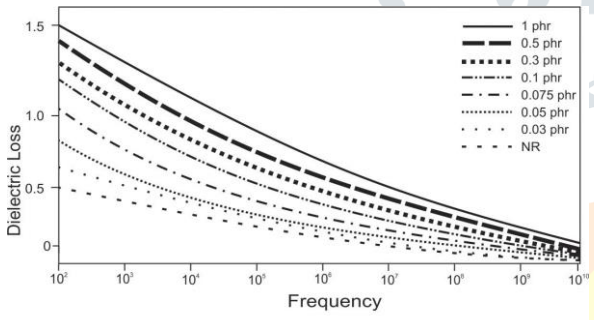

(c)

Fig. 9 Dielectric properties as a function of frequency
(a) AC conductivity (b) dielectric constant
(c) dielectric loss for NR-GO Nanocomposites.

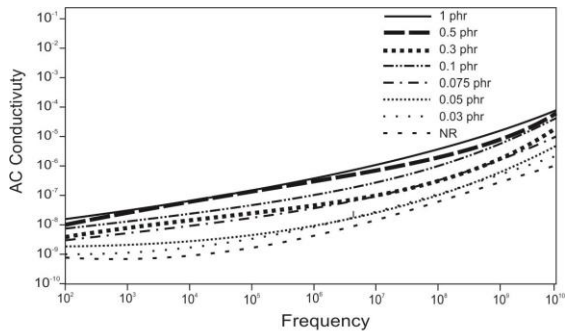

(a)

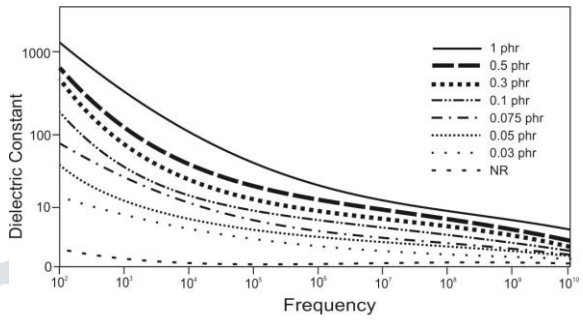

(b)

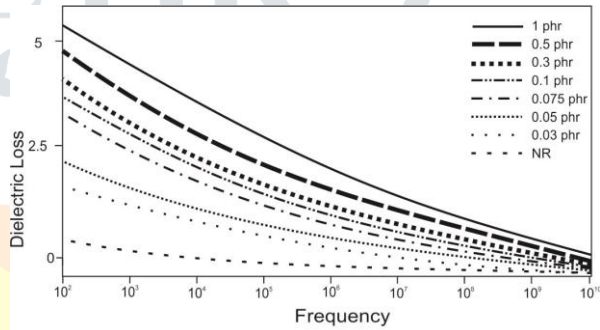

(c)

Fig. 10 Dielectric properties as a function of frequency
(a) AC conductivity (b) dielectric constant
(c) dielectric loss for NR- RGO Nanocomposites

4. CONCLUSIONS

RGO synthesized from GO was characterised by XRD, FTIR, UV, SEM and TEM. NR-RGO nanocomposites of varying compositions were prepared by latex mixing method. These composites were characterised by XRD and SEM. The uniform dispersion of RGO, together with its strong interaction with NR, makes a great contribution to improvement in the tensile properties for the NR- RGO nanocomposites at very low filler loading. With incorporation of as little as 0.1 phr of RGO, 69 % increase in the tensile strength and 84 % increase in the initial tensile modulus are achieved without sacrificing the ultimate strain. NR- RGO nanocomposite also showed enhancement in dielectric properties. The better mechanical and dielectric properties of the composites confirms RGO as good nanofiller than GO. We can conclude that the use of RGO as a filler in NR can overcome some of the disadvantages of NR and can produce high quality NR nanocomposites. Also RGO with its unique properties can be utilised for a range of applications and show excellent promise as reinforcing agent in elastomeric nanocomposites. The versatile properties make the NR-RGO nanocomposites a promising new class of advanced materials, which can be used in green tires and electronic skin.

Conflicts of Interest

There are no conflicts of interest to declare.

5. ACKNOWLEDGEMENT

The authors would like to thank the Research Department of Chemistry Maharajas College, Ernakulam and Department of Polymer science and Rubber Technology, Cochin University Of Science And Technology, for providing facilities for doing this work.

References

1) De SK, White JR (2001) "Rubber technologist's handbook", Smithers Rapra Technology, New York.

2) M.P. Wagner (1976) Reinforcing Silica and Silicates, Rubber Chem. Technol. 49, p 703–775.

3) Medalia AI (1978) "Effect of carbon black on dynamic properties of rubber vulcanizates", Rubber Chem Technol. 51(3):437–523.

4) Balandin AA, Ghosh S, Bao W, Calizo I, Teweldebrhan D, Miao F, et al. (2008) "Superior Thermal Conductivity of Single-Layer Graphene",Nano Letters.8(3):902-7.

5) Novoselov KS, Geim AK, Morozov SV, Jiang D, Zhang Y, Dubonos SV, et al. (2004) "Electric Field Effect in Atomically Thin Carbon Films", Science. 306(5696):666-9.

6) Lee C, Wei X, Kysar JW, Hone J. (2008) "Measurement of the elastic properties and intrinsic strength of monolayer graphene", Science. 321(5887):385-8.

7) Putz KW, Compton OC, Palmeri MJ, Nguyen ST, Brinson LC. (2010) "High-Nanofiller-Content Graphene Oxide-Polymer Nanocomposites via Vacuum-Assisted Self-Assembly", Advanced Functional Materials.;20(19):3322-9.

8) Potts JR, Dreyer DR, Bielawski CW, Ruoff RS. (2011) "Graphene-based polymer nanocomposites", Polymer.;52(1):5-25.

9) K. K. Sadasivuni, D. Ponnamma, S. Thomas, and Y. Grohens, (2014) "Evolution from graphite to graphene elastomer composites," Progress in Polymer Science. vol. 39, no. 4, pp. 749–780.

10) Stankovich S., Dikin D. A., Dommett G. H. B., Kohlhaas K. M., Zimney E. J., et al. (2006) "Graphene-based composite materials", Nature.; 442 (7100): 282–286.

11) Ozbas B, O'Neill CD, Register RA, Aksay IA, Prud'homme RK, Adamson DH. (2012) "Multifunctional elastomer nanocomposites with functionalized graphene single sheets", J Polym Sci Polym Phys.;50(13):910–6.

12) Prud'HommeRK, OzbasB, AksayI,Register R,Adamson D.(2010) "Functionalgraphene rubber nanocomposites". In: Patent US, editor. United States Patent, vol. US7745528B2. US: The Trustees of Princeton University;. p. 1–80.

13) Tang Z, Wu X, Guo B, Zhang L, Jia D. (2012) " Preparation of butadiene–styrene–vinyl pyridine rubber–graphene oxide hybrids through co-coagulation process and in situ interface tailoring", J Mater Chem.;22(15):7492–501.

14) Zhan Y, Lavorgna M, Buonocore G, Xia H. (2012) "Enhancing electrical conductivity of rubber composites by constructing interconnected network of self-assembled graphene with latex mixing", J Mater Chem.;22(21):10464–8.

15) Lee C, Wei X, Li Q, Carpick R, Kysar JW, Hone J. (2009) "Elastic and frictional properties of graphene", physica status solidi (b).;246(11-12):2562-7.

16) Hummers, W. S.; Offeman, R. E. J Am, (1958) "Preparation of graphite oxide", Chem Soc., 80, 1339–1339.

17) Sungjin Park, Jinho An, Jeffrey R. Potts , Aruna Velamakanni , Shanthi Murali , Rodney S. Ruoff. (2011) "Hydrazine-reduction of graphite- and graphene oxide", CARBON 49 3019 – 3023

18) C. F. Flint and W. J. S. Naunton, (1937,) "Physical Testing of Latex Films, Rubber Chemistry and Technology", September, Vol. 10, No. 3, pp. 584-614.

19) Ning Cao and Yuan Zhang. (2015) "Study of Reduced Graphene Oxide Preparation by Hummers' Method and Related Characterization", Journal of Nanomaterials. Volume, pp-168125

20) Wu S, Tang Z, Guo B, Zhang L, Jia D. (2013) "Effects of interfacial interaction on chain dynamics of rubber/graphene oxide hybrids: a dielectric relaxation spectroscopy study", RSC Adv;3(34):14549–59.

21) 21. I.Childres, (2013)"Raman spectroscopy of graphene and related materials",Book, ,ch.19.

22) Zhao G. K., Li X. M., Huang M. R., Zhen Z., Zhong Y. J., et al. (2017) "The physics and chemistry of graphene-on-surfaces", Chemical Society Reviews. 46 (15): 4417–4449.

23) Allen, M.J., Tung, V.C., and Kaner, (2010) "Honeycomb Carbon : A Review of Gaphene" Chem. Rev,Volume 110, pp-132

24) Kuilla T., Bhadra S., Yao D. H., Kim N. H., Bose S., and Lee J. H. (2010) "Recent advances in graphene based polymer composites", Progress in Polymer Science. 35 (11): 1350–1375.

25) Wang, Z.H.; Liu, J.; Wu, S.Z., Wang, W.C.; Zhang, L.Q. (2010,) "Novel percolation phenomena and mechanism of strengthening elastomers by nanofillers". Phys. Chem. Chem. Phys. 12, 1.

26) Balandin A. A., Ghosh S., Bao W. Z., Calizo I., Teweldebrhan D., et al. (2008;) "Superior thermal conductivity of single-layer graphene", Nano Letters. 8 (3): 902–907.

27) Zhan Y, Lavorgna M, Buonocore G, Xia H. (2012;) "Enhancing electrical conductivity of rubber composites by constructing interconnected network of self-assembled graphene with latex mixing" J Mater Chem. 22(21):10464–8.

28) Araby S, Zhang L, Kuan H-C, Dai J-B, Majewski P, Ma J. (2013) "A novel approach to electrically and thermally conductive elastomers using graphene", Polymer;54(14):3663–70.